



Short communication

Surface barrier analysis of semi-insulating and n^+ -type GaAs(001) following passivation with n -alkanethiol SAMs

Gregory M. Marshall^{a,b}, Farid Bensebaa^b, Jan J. Dubowski^{a,*}

^a Laboratory for Quantum Semiconductors and Photon-Based BioNanotechnology, Department of Electrical and Computer Engineering, Université de Sherbrooke, Sherbrooke, Québec, J1K 2R1, Canada

^b Institute for Chemical Process and Environmental Technology, National Research Council of Canada, Ottawa, Ontario, K1A 0R6, Canada

ARTICLE INFO

Article history:

Received 23 June 2010

Received in revised form

14 December 2010

Accepted 15 December 2010

Available online 21 December 2010

Keywords:

Self-assembled monolayers

X-ray photoelectron spectroscopy

Surface Fermi level

GaAs

ABSTRACT

The surface Fermi level of semi-insulating and n^+ -type GaAs(001) was determined before and after passivation with n -alkanethiol self-assembled monolayers (SAMs) by X-ray photoelectron spectroscopy. Fermi level positioning was achieved using Au calibration pads integrated directly onto the GaAs surface, prior to SAM deposition, in order to provide a surface equipotential binding energy reference. Fermi level pinning within 50 meV and surface barrier characteristics according to the Advanced Unified Defect Model were observed. Our results demonstrate the effectiveness of the Au integration technique for the determination of band-edge referenced Fermi level positions and are relevant to an understanding of emerging technologies based on the molecular–semiconductor junction.

© 2010 Elsevier B.V. All rights reserved.

1. Introduction

Knowledge of the surface barrier height is fundamental to the development of junction-based semiconductor devices, a unique class of which has emerged based on surface chemical architectures for molecular junction and various sensor applications. In this context, and as a fundamental material science, n -alkanethiol [HS-(CH₂) _{n} -CH₃] self-assembled monolayers (SAMs) have been investigated for their ability to provide a passivating interface to GaAs(001) through S–GaAs covalent bond formation [1–5]. A characteristic parameter of the resulting barrier height is the surface Fermi level (FL).

In this letter, we report on the use of X-ray photoelectron spectroscopy (XPS) to establish the equilibrium position of the GaAs(001) surface FL before and after the formation of n -alkanethiol SAMs. Measurements of the relative change of the surface FL upon passivation of GaAs(001) with alkanethiols have been made using Raman spectroscopy [6,7], a technique that obtains the band-bending from estimated changes in the depletion depth. These experiments are subject to uncertainty introduced by the establishment of a surface photovoltage, which screens differences in the equilibrium surface barrier, and that may be substantial

owing to the large irradiances required to obtain a Raman signal. Moreover, the Raman technique does not provide a band-edge referenced position of the surface FL. XPS methods have been used for this purpose on doped substrates, by reference to an external Au film using UV photoelectron spectroscopy, but relative FL changes upon passivation with the SAM were not reported [8]. In semi-insulating (SI) GaAs, the native barrier height is supported by lower surface charge densities, relative to doped material, providing a more sensitive platform on which to investigate SAM-induced FL effects. However, external FL referencing requires equipotential contact between the sample and the calibrant, usually via the spectrometer ground, which is difficult to obtain for a SI material. Post-process Au decoration can circumvent the insulating barrier, providing an internal surface equipotential reference [9], but overlying may damage the ordered molecular structure of the SAMs, and would not provide direct contact with the GaAs substrate. In order to avoid these issues, Au binding energy reference pads were integrated directly onto the GaAs surface before SAM deposition as an effective approach to FL calibration at the molecular junction.

2. Experimental

Undoped SI and n^+ -type (Si-doped at $1 \times 10^{18} \text{ cm}^{-3}$) GaAs(001) wafers were used for this study. Integrated Au reference pads were evaporated on etched GaAs surfaces, following UV photolithography on PMMA photoresist, with diameters of about 170 μm and thicknesses in excess of 50 nm. Details on the preparation of hex-

* Corresponding author. Tel.: +1 819 821 8000x62528; fax: +1 819 821 7937.

E-mail address: jan.j.dubowski@usherbrooke.ca (J.J. Dubowski).

URL: <http://www.dubowski.ca> (J.J. Dubowski).

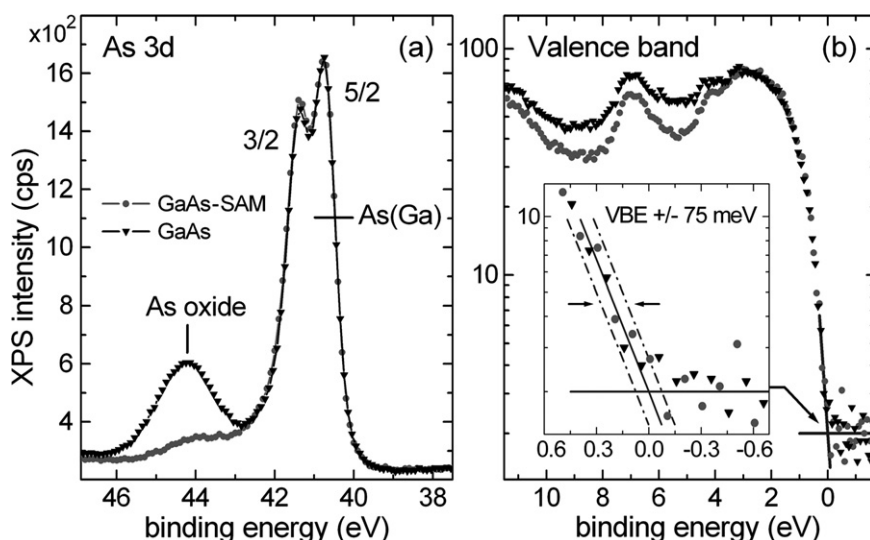


Fig. 1. XPS As 3d core level (a) and valence band (b) regions of Si-GaAs for samples: (circles) passivated with HDT SAM, and (triangles) etched only and reoxidized. Spectra are referenced to the VBE (solid line intersection), determined by extrapolation in the logarithmic domain. GaAs phase As 3d peaks are labeled with spin-orbit branching. Photoelectron take-off angle: 90° .

adecanethiol (HDT) [$\text{HS}-(\text{CH}_2)_{15}-\text{CH}_3$] SAMs have been reported elsewhere [10]. In order to provide a stabilized control, etched only GaAs wafers were allowed to reoxidize in air briefly (~ 3 min). Samples prepared with SAMs were transferred directly to the XPS vacuum chamber from the N_2 environment in which they were prepared, with only a few seconds of ambient exposure.

3. Results and discussion

3.1. X-ray photoelectron spectroscopy

The As 3d core level and valence band regions are plotted in Fig. 1(a) and (b), for both SAM prepared and etched/reoxidized Si-GaAs surfaces. The As 3d core levels are shown calibrated such that the zero of binding energy corresponds to the valence band-edge (VBE), which was estimated by visual extrapolation in the logarithmic domain to a precision of ± 75 meV. Note that the GaAs density of states (XPS intensity) converges to the same zero for both sample types. Therefore, a constant VBE referenced core level energy (As $3d_{\text{VBE}}$) is validated. Specifically, we referenced the well-resolved As $3d_{5/2}$ spin-orbit branch by spectral decomposition and obtained a value of 40.73 eV. Application of the As $3d_{\text{VBE}}$ energy for the determination of GaAs surface FLs has been previously demonstrated [8,11].

XPS spectra were also recorded in the Au 4f region where the FL was referred to the Au $4f_{7/2}$ line, as indicated in Fig. 2(a), which provides a stable FL reference at 84.00 eV [12]. Complementary O 1s spectra are plotted in Fig. 2(b). The O 1s spectra were collected at a 30° photoelectron take-off angle in order to emphasize surface oxide concentrations in contrast to the 90° take-off used for the other measurements. The O 1s panel shows the oxide level associated with the etched/reoxidized reference wafer (upper series) and the null oxide level following SAM passivation (lower series). The shape of the O 1s region background near 532 eV is due to a periodic Ga LMM Auger feature, observable after cleaving under vacuum conditions [13], and thereby demonstrates, within the limit imposed by this background, that the surface oxide concentration is negligible.

When the Au and GaAs materials are equipotential, a measurement of the difference between the Au $4f_{7/2}$ and As $3d_{5/2}$ uncalibrated core level energies (Δ_{XPS}) yields the calibrated position of the GaAs surface FL in terms of the energy (E_f) above the VBE

as follows, $E_f = 84.00 - \Delta_{\text{XPS}} - \text{As } 3d_{\text{VBE}}$. This calibration is graphically represented in the energy level diagram of Fig. 3. Note that this method is insensitive to work function differences that may arise from oxidation, surface dipoles associated with the SAM, or the effect of any thiol adsorption on the Au pads. In order to verify that the two materials were equipotential, biasing applied by a charge neutralization (C/N) current (thermionic emission) shifted the core levels up to 1.1 eV, where it was observed that Δ_{XPS} remained constant within normal peak fitting error (≤ 40 meV). In addition, GaAs spectra were recorded laterally separate from and immediately adjacent to the Au pads (relative to the $300 \mu\text{m} \times 700 \mu\text{m}$ XPS field of view), and were found to have equivalent peak energy positions, with and without bias shifting applied. Moreover, since the Au pads were made to a thickness (50 nm) much greater than the XPS sampling depth (~ 5 nm), any band-bending variation directly below the Au pads was not detected in the measurement. Therefore, it was sufficient to verify spectral invariance and potential uniformity laterally on the surface.

Table 1 (col. 7) lists the FL results for both SI and n^+ substrate types, based on a calculation of E_f using the uncalibrated energies in cols. 2–5. In col. 6, no significant difference in Δ_{XPS} is observed,

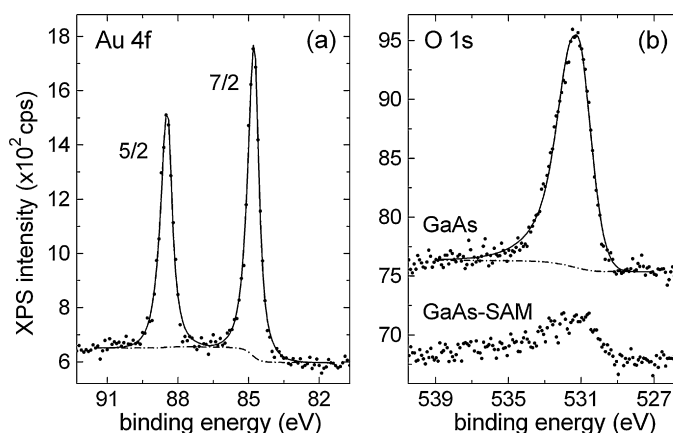


Fig. 2. XPS spectra. (a) Au 4f peaks labeled with spin-orbit branching. (b) The O 1s region includes spectra following passivation with HDT SAM (lower series) and from the etched and reoxidized GaAs reference surface (upper series), shifted vertically for clarity. Spectra are not energy calibrated. Photoelectron take-off angles: Au 4f, 90° ; O 1s, 30° .

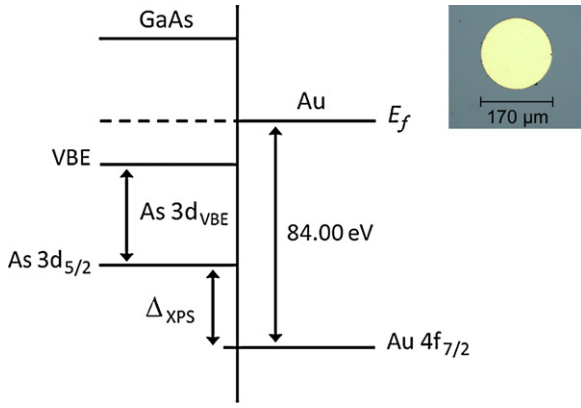


Fig. 3. Energy level diagram illustrating the XPS binding energy referencing used in order to determine the surface FL position above the VBE. Core levels refer to the spin-orbit components identified in Figs. 1 and 2. Inset: optical image showing a Au calibration pad integrated onto the GaAs surface.

Table 1

Evaluation of the VBE referenced surface FL in SI and n^+ -doped GaAs(001) prepared with $[\text{HS}-(\text{CH}_2)_{15}-\text{CH}_3]$ SAMs using Au XPS core level calibration.

Sample type	C/N off		C/N on		δ (eV)	E_f (eV)
	As 3d _{5/2}	Au 4f _{7/2}	As 3d _{5/2}	Au 4f _{7/2}		
SI-GaAs (Ref)	41.61 ^a	84.67	40.96	83.99	-0.03 ^b	0.21 ^c
SI-GaAs (SAM)	41.74	84.75	40.62	83.61	-0.02	0.26
n^+ -GaAs (Ref)	41.79	84.37	41.66	84.26	0.02	0.69
n^+ -GaAs (SAM)	41.80	84.35	41.65	84.24	0.04	0.71

^a Columns 2–5, uncalibrated XPS binding energy in eV.

^b Variation of GaAs–Au peak separation (Δ_{XPS}) with up to 1.1 eV bias.

^c Values calculated from columns 2 and 3. Estimated error ± 90 meV.

with and without C/N biasing applied, confirming the equipotential contact between the GaAs and Au materials. In subsequent tests, E_f repeatability within 60 meV was observed, which accords with the given uncertainties. As a relative measure of error, repeatability within 10 meV specific to the increase in E_f after thiol treatment was obtained. Table 1 indicates that the passivating effect of n -alkanethiol SAMs is limited to a 50 meV reduction in equilibrium band-bending for SI-GaAs and a 20 meV reduction for n^+ -type GaAs, i.e., a strong pinning effect is realized.

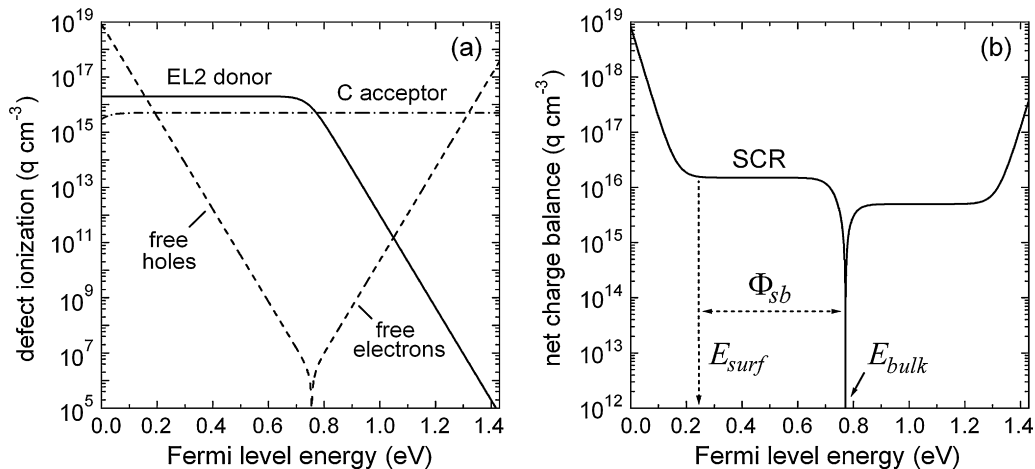


Fig. 4. (a) Ionized charge centre concentrations for the EL2 donor (solid) and carbon acceptor (dotted) defect levels in undoped SI-GaAs. Free carrier concentrations as indicated (dashed). (b) Net charge balance. The zero of charge marks the bulk Fermi level energy (E_{bulk}). The surface FL (E_{surf}) is determined experimentally and defines the surface potential barrier (Φ_{sb}) and limit of ionization in the space charge region (SCR).

3.2. Validation of the Fermi level results

In conjunction with known mechanisms of bulk charge balance and the Advanced Unified Defect Model (AUDM) of the GaAs surface [14], the characteristic parameters of the surface barrier are now analyzed in order to verify the accuracy of the FL measurements. In bulk GaAs material, the EL2 defect is attributed to As_{Ga} antisites, which in undoped SI-GaAs is compensated by extrinsic impurities such as carbon, a shallow level acceptor [15,16]. As demonstrated below, this mechanism yields the intrinsic-like character in undoped material. In the AUDM, the EL2 is a deep double donor, with levels around 0.75 eV and 0.50 eV above the VBE. These donors, along with shallow level acceptors in the surface region, often attributed to Ga_{As} antisite defects, are required for mid-gap surface pinning in n -doped material. Moreover, the AUDM specifies that the surface FL shifts from the mid-gap closer to the VBE by up to 0.5 eV when the surface is Ga-rich, a shift more easily accommodated in SI-GaAs without an extrinsic n -type donor [14]. In agreement with the AUDM, Table 1 (col. 7) shows that the surface FL exists at E_f values of 0.69 eV for n^+ -type GaAs and 0.21 eV for SI material, which we observe to be about 15% Ga-rich (XPS atomic percent) after $\text{NH}_4\text{OH}/\text{H}_2\text{O}$ etching similarly with Ref. [17]. Our results also concur with evidence of a surface acceptor state at 0.27 eV in undoped SI-GaAs that was found using photothermal radiometric deep-level transient spectroscopy [18].

The surface barrier of SI-GaAs can now be characterized in terms of the ionized charge concentrations (Q_{dd} and Q_{sa}) and the net concentration of free carriers (ΔQ_{fc}) expressed as a function of the FL energy (E_f). These terms are based on typical values for the volume concentration, degeneracy factor and activation energies of the EL2 deep donor (N_{dd} , g_{dd} , E_{dd}) and carbon shallow acceptor (N_{sa} , g_{sa} , E_{sa}) defects [15,16].

$$\Delta Q_{\text{fc}}(E_f) = 2qn_i \sinh \frac{E_i - E_f}{kT} \quad (1)$$

$$Q_{\text{dd}}(E_f) = \frac{qN_{\text{dd}}}{1 + g_{\text{dd}} \exp[(E_f - E_{\text{dd}})/kT]} \quad (2)$$

$$Q_{\text{sa}}(E_f) = \frac{qN_{\text{sa}}}{1 + g_{\text{sa}} \exp[(E_{\text{sa}} - E_f)/kT]} \quad (3)$$

The degeneracy factor is the ratio $g = g_0/g_1$, where the g_i are the degeneracies of the defect state when occupied by $i = 0, 1$ electrons, q is the elementary charge unit, k is the Boltzmann constant, T is the absolute temperature, and the value n_i is the intrinsic carrier concentration for GaAs. The intrinsic FL energy (E_i) is determined

from the ratio of electron/hole effective masses $r_m = m_n^*/m_p^*$ in the expression $2E_i = E_g - (3/2)kT \ln r_m$, where E_g is the band-gap energy. Eqs. (1)–(3) are plotted in Fig. 4(a). The net charge balance for the values assumed is shown in Fig. 4(b) and is obtained by evaluating the sum,

$$\sum Q(E_f) = |\Delta Q_{fc}(E_f) + Q_{dd}(E_f) - Q_{sa}(E_f)| \quad (4)$$

yielding an intrinsic-like bulk FL position of 0.77 eV at the charge balance zero, to which the surface barrier is referred. Fig. 4(b) also indicates that, for SI-GaAs, the excess charge density is $1.5 \times 10^{16} \text{ cm}^{-3}$, which is attributed to a uniform space charge region in depletion resulting from ionization of the native defects. We also observe why filling of the surface acceptor states is limited by native defect ionization in SI-GaAs; a charge balance in excess of the ionized defect concentration would imply a further reduction of the surface FL, which is energetically unfavorable, since the surface states would need to fill from the valence band in this case.

4. Conclusions

XPS determination of the VBE referenced surface FL position following passivation with *n*-alkanethiol SAMs revealed that unpinning of the surface FL was limited to less than 50 meV. This result validates recent calculations indicating that complete passivation of the available surface sites is sterically hindered by the SAM [19]. For SI-GaAs, the surface FL was located at 0.26 eV above the VBE, which is indicative of a high concentration of surface acceptor states and a barrier height of 0.51 eV consistent with both a Ga-rich stoichiometry and ionization of the EL2 defect in its typical bulk concentration ($\sim 10^{16} \text{ cm}^{-3}$). Similarly, the n^+ -GaAs surface barrier was determined to be 0.76 eV based on a surface FL located at 0.71 eV and ionization in the space charge region specified by the nominal doping concentration.

Acknowledgements

Funding for this research was provided by the joint NanoQuébec – Canadian Institute for Photonic Innovation – Canadian Space Agency Support Program for Integrative Biosensor Research, the Canada Research Chair in Quantum Semiconductors Program and the National Research Council of Canada Graduate Student Scholarship Supplement Program.

References

- [1] C.L. McGuiness, A. Shaporenko, C.K. Mars, S. Uppili, M. Zharnikov, D.L. Allara, *J. Am. Chem. Soc.* 128 (2006) 5231.
- [2] A. Ahktari-Zavareh, W. Li, K.L. Kavanagh, A.J. Trionfi, J.C. Jones, J.L. Reno, J.W.P. Hsu, A.A. Talin, *J. Vac. Sci. Technol. B* 26 (2008) 1597.
- [3] K. Lee, G. Lu, A. Facchetti, D.B. Janes, T.J. Marks, *Appl. Phys. Lett.* 92 (2008) 123509.
- [4] D.G. Wu, D. Cahen, P. Graf, R. Naaman, A. Nitzan, D. Shvarts, *Chem. Eur. J.* 7 (2001) 1743.
- [5] J.J. Dubowski, O. Voznyy, G.M. Marshall, *Appl. Surf. Sci.* 256 (2010) 5714.
- [6] J.F. Dorsten, J.E. Maslar, P.W. Bohn, *Appl. Phys. Lett.* 66 (1995) 1755.
- [7] C.L. McGuiness, A. Shaporenko, M. Zharnikov, A.V. Walker, D.L. Allara, *J. Phys. Chem. C* 111 (2007) 4226.
- [8] G. Neshet, A. Vilan, H. Cohen, D. Cahen, F. Amy, C. Chan, J. Hwang, A. Kahn, *J. Phys. Chem. B* 110 (2006) 14363.
- [9] D.A. Stephenson, N.J. Binkowski, *J. Non-Cryst. Solids* 22 (1975) 399.
- [10] G.M. Marshall, F. Bensebaa, J.J. Dubowski, *J. Appl. Phys.* 105 (2009) 094310.
- [11] R.W. Grant, J.R. Waldrop, S.P. Kowalczyk, E.A. Kraut, *J. Vac. Sci. Technol.* 19 (1981) 477.
- [12] NIST X-ray Photoelectron Spectroscopy Database, Version 3.5, 2003.
- [13] D.M. Poirier, J.H. Weaver, *Surf. Sci. Spectra* 2 (1993) 201.
- [14] W.E. Spicer, Z. Liliental-Weber, E. Weber, N. Newman, T. Kendelewicz, R. Cao, C. McCants, P. Mahowald, K. Miyano, I. Lindau, *J. Vac. Sci. Technol. B* 6 (1988) 1245.
- [15] G.M. Martin, J.P. Farges, G. Jacob, J.P. Hallais, G. Poiblaud, *J. Appl. Phys.* 51 (1980) 2840.
- [16] R.B. Darling, *J. Appl. Phys.* 74 (1993) 4571.
- [17] T. Aqua, H. Cohen, A. Vilan, R. Naaman, *J. Phys. Chem. C* 111 (2007) 16313.
- [18] A. Mandelis, R.A. Budiman, *Superficies Y Vacio* 8 (1999) 13.
- [19] O. Voznyy, J.J. Dubowski, *Langmuir* 24 (2008) 13299.